Supplemental Materials

Molecular Biology of the Cell

Bottanelli et al.

Supplementary information

Note 1: Estimate of the density of ARF1 on Golgi-derived tubules (Table 1)

To be able to estimate the number of ARF1 molecules on tubules we took advantage of two fluorescent internal standards:

1) COPI vesicles in the β-COP^{EN}-SNAP cell line. From a published cryo-EM structure we know that each COPI vesicle with 35 nm diameter contains around 72 copies of ARF1, with one ARF1 molecule covering a surface of ~50.4 nm^2 (Dodonova et al., 2015). A vesicle in a living cell (diameter ~75 nm surface=17.662 nm^2) should contain ~350 ARF1 molecules. It is known that ARF1 and coatomer are present on vesicles at a stoichiometric ratio of 2:1. Therefore vesicles will contain around 350/2=175 β-COP molecules. We then determined from western blot (Figure 5d) that the amount of tagged β-COP^{EN}-SNAP represents ~85% of the total amount of β-COP. Therefore if we label β-COP^{EN}-SNAP cells with SiR-BG, we estimate the number of fluorphores per vesicle to be ~150.

We drew 200 nm * 200 nm boxes around putative COPI vesicles/buds and ARF1^{EN}-Halo-positive tubules in β-COP^{EN}-SNAP cells labeled with SiR-BG and ARF1^{EN}-Halo labeled with SiR-CA and measured fluorescent intensities of the two structures. We assume that the labeling efficiency of SNAP and Halo tag is comparable and close to 100% for both tags. The fluorescence intensity of the tubules is 2.2 ± 1.5 times the intensity of the vesicles. We know that this fluorescence intensity corresponds to around 150 fluorophores in the case of COPI vesicles and can therefore infer that each 200 nm long tubule fragment contains around 150*2.2=330 ARF1^{EN}-Halo molecules and a total of around 330*5=1650 molecules per µm length of tubule. If we then consider that the ARF1^{EN}-Halo cell line is heterozygous and only half of the ARF1 molecules are tagged and fluorescent we can estimate that each µm of tubule is coated with 1650*2=3300 ARF1 molecules. The surface of 1 µm long tube with a diameter of ~110 nm (Fig. 1g) is around 0.34 µm^2. In summary, the density of ARF1 on the tubules is estimated to be ~10,000 ARF1/µm^2 with one ARF1 molecule covering an area of ~104 nm^2.

2) Microtubules labeled with SiR-tubulin.

The number of tubulin subunits/µm of microtubule length is estimated to be ~1750 (Cooper et al., 2010).

We drew boxes of 400nm * 1000nm along microtubules labeled with SiR-tubulin and ARF1^{EN}-Halo tubules labeled with SiR-CA. Again we assume that 1 SiR-tubulin molecule binds to 1 tubulin subunit and that the labeling efficiency of Halo tag is close to 100%. The intensities measured for ARF1^{EN}-Halo tubules were 2.1 ± 0.7 times higher than for microtubules. We can therefore estimate that the amount of fluorescent ARF1^{EN}-Halo molecules on a µm of tubule is around 1750*2.1=3675. Again the ARF1^{EN}-Halo cell line is heterozygous so the total amount of ARF1 on the tubules is around 3675*2=7350. In summary, the density of ARF1 on the tubules is estimated to be around 20,000 ARF1/µm^2 with one ARF1 molecule covering an area of around 47 nm^2.

Note 2: Estimate of the contribution of ARF1 tubules on the membrane flow of the cell

Membrane flow out of the ER
155 COPII vesicles/sec (Barlowe and Helenius, 2016; Thor et al., 2009)
Average radius (r) of a COPII vesicle = 30 nm (Barlowe et al., 1994)
Surface of a COPII vesicle=0.011 μm^2
155(frequency)*0.011(surface)=1.7 μm^2/sec=**~6138 μm^2/hour**

Flow of retrograde ARF1^{EN}-Halo tubules
Average r=0.055 µm and length=2.9 ± 1.6 µm
Surface of the average tubule=1 μm^2
Frequency of retrograde tubules=1.26 tubules/min (Figure 6)
Surface imaged (single confocal plane) vs whole surface of the Golgi in HeLa cells=1:4.8
Corrected frequency of retrograde tubules=6 tubules/min
6(tubules/min)*1(surface)*60=**~360 μm^2/hour or ~6% of the flow out of the ER or ~7% of the area needed to return to ER to maintain membrane balance**

Flow of anterogarde ARF1^{EN}-Halo tubules
Frequency of anterograde tubules=3.05 tubules/min (Figure 5)
Corrected frequency of anterograde tubules=14.6 tubules/min
14.6(tubules/min)*1(surface)*60=**~878 μm^2/hour or 14% of the flow out of the ER**

Supplementary methods

Recombinant Plasmids

ARF1-GFP and ARF1-Q71L-GFP (Vasudevan et al., 1998), SNAP-CLC and ManII-SNAP (Bottanelli et al., 2016), GFP-FM4-GPI (Deng et al., 2016), secHRP (Connolly et al., 1994) YFP-ERGIC53 (Hamlin et al., 2014) and VSV G-GFP (Presley et al., 1997) were described previously.

ARF1-Halo was generated by linearizing ARF1-GFP (Vasudevan et al., 1998) with BamHI and NotI and ligating Halo tag as a BamHI-NotI fragment. Halo was amplified with the following oligos: Halo- sense 5'-TAGCGGGATCCAGGCTCAGGTTCTGGAATGGCAGAAATCGGTACTGGCTTTCC-3' and Halo- anti 5'-TGCAATGCGGCCGCTCAGCCGGAAATCTCGAGCGTCGACAGCC-3'.

KDEL-R-SNAP (hERD2-SNAP) was generated by linearizing pEGFP-N1 with EcoRI and NotI and inserting KDEL-R and SNAP tag as EcoRI-BamHI and BamHI-NotI fragments. KDEL-R was amplified with the following oligos: KDEL-R-sense 5'-ATCGAGAATTCATGAATCTCTTCCGATTCCTGGGAGACCTC-3' and KDEL-R-anti 5'-CGTATGGATCCCGTGATCCTGAACCAGATCCTGCCGGCAAACTCAACTTCTTCCCCTTTAGGAC-3'. SNAP tag was amplified with the following oligos SNAP-sense 5'-GCTCGGGATCCACCGGTCGCCACCATGGACAAAGACTGCGAAATGAAGCGC-3' and SNAP-anti 5'-GTCCTAGCGGCCGCTCAACCCAGCCCAGGCTTGCCCAGTCTG-3'.

VSV G-SNAP was generated by linearizing the VSV G-GFP plasmid (Presley et al., 1997) with BamHI and NotI and inserting Halo tag as a BamHI-NotI fragment as described for KDEL-R-SNAP.

To generate Halo-CLC, Halo tag was fused to the N-terminus of Clathrin Light Chain as described in Bottanelli et al., 2016 for SNAP-CLC.

CRISPR/Cas9 Gene editing

The ARF1 genomic locus (Gene ID 375) was targeted with the following guide RNA: 5'-CCACATGAGAGTAAAGCAGAGGG-3' (PAM sequence is underlined) located just after the stop codon in the ARF1 coding sequence. This guide RNA does not have off-target matches, as tested using the CRISPR design tool from the Zhang lab website (http://crispr.mit.edu). The guide RNA was cloned into the SpCas9 pX330 plasmid (addgene plasmid #42230) (Cong et al., 2013) by annealing oligos and ligating them into the vector, previously linearized with BbsI. Two oligos (ARF1-sense 5'-ACCTCCCCAACGCCATGAATGCGG-3' and ARF1-anti 5'-TGCTAGGCGGGGTCTCCC-3') were used to amplify the genomic region around the cut and then to genotype potential clones. The homologous repair plasmid to generate gene edited ARF1-Halo was constructed starting from the pEGFP-N1 plasmid. First Halo was clones into pEGFP-N1 using the oligos Halo-sense 5'-TAGCGGGATCCAGGCTCAGGTTCTGGAATGGCAGAAATCGGTACTGGCTTTCC-3' and Halo-anti 5'-

TGCAATGCGGCCGCTCAGCCGGAAATCTCGAGCGTCGACAGCC-3' and the BamHI/NotI restriction sites. Then the right homology arm (~1 Kb) was cloned into pHalo-N1 after the Neo^r/Kan^r resistance cassette using EcoO109I to integrate the whole cassette and allow selection of positive recombinants with the drug G418/Geneticin (Thermo Fisher Scientific). The left homology arm (~1 Kb) was the cloned using the AseI and BamHI sites. The PAM site was mutagenized to avoid re-cutting by the Cas9. A glycin/serin rich linker was added (GSSGRDPGSGSG). SNAP and GFP were then cloned into the full HR plasmid as BamHI/NotI fragments.
The pX330 plasmid with the ARF1 guide and the homologous recombination plasmid were transfected in HeLa CCL-2 cells and HAP1 cells using Lipofectamine 2000. G418 was added to the cells a week after transfection. After two weeks of selection cells were subjected to fluorescent-activated cell sorting (FACS) to obtain single clones. Clones were genotyped via western blot and PCR using the ARF1-sense and ARF1-anti oligos. All the ARF1 clones were heterozygous. This may be due to the fact that the ARF1 locus is on chromosome 1 which could be present in 3 copies in HeLa cells. For the selected clones used in this paper the whole ARF1 genomic locus was amplified via PCR and sequenced using an ARF1-locus-sense oligo 5'-CTTTCTGGCCATGCAGCTGTGG-3' and a polyA-anti oligo 5'-GTTTGGACAAACCACAACTAGAATGC-3'. The untagged allele was also PCR amplified and sequenced to confirm no mutations were inserted in the coding sequence.
The last exon of the COPB1 gene (gene ID 1315) was targeted with the following guide RNA 5'-CAGGGAATGGCCTTAAGTCTTGG-3'. Again the gRNA was tested for off-target matches as above. The gRNA was inserted into a scaffold that bears all components necessary for gRNA expression (Mali et al., 2013). To test for the appropriate cut of the last exon by the gRNA the Surveyor Mutation Detection Kit (Transgenomics) was used according to manufacturer's guidelines. The homologous repair plasmid was synthetized by GenScript and contains 500 bp long right and left homology arms. A linker (GHGTGSTGSGSS) was added between the C-terminus of the COPB1 gene and the SNAP tag.
The homologous recombination plasmid, the human Cas9 plasmid (Addgene plasmid #41815) and the pCR-Blunt II-TOPO vector (Invitrogen) encoding for the gRNA were transfected into HeLa CCL-2 cells using the Nucleofect transfection kit (Lonza). Again, single clones were isolated using FACS. Clones were validated via western blotting, fluorescent microscopy, and exon sequencing was carried out on the clone used in this study. For the untagged allele, non-homologous end joining caused a deletion of 7 bp, which resulted in a protein that is 12 amino acids longer. However the protein is unstable making the β-COP^{EN}-SNAP cell line almost homozygous at the protein level.

Electron Microscopy
Cells grown in petri dishes were fixed in 2.5% gluteraldehyde in 0.1M sodium cacodylate buffer pH7.4 for 1 hour, then rinsed in buffer and were spun down in 2% agar in 0.1M sodium cacodylate. The chilled blocks were trimmed and post

fixed in 1% osmium tetroxide for 1 hour, then *en bloc* stained in aqueous 2% uranyl acetate for a further hour, then rinsed in buffer and dehydrated in an ethanol series from 50% to 100%. The samples were infiltrated with Embed 812 (Electron Microscopy Sciences) epoxy resin and baked overnight at 600 °C. Hardened blocks were cut using a Leica UltraCut UC7. 60nm sections were collected on formvar/carbon coated grids and contrast stained using 2% uranyl acetate and lead citrate. Grids were viewed FEI Tencai Biotwin TEM at 80Kv. Images were taken using Morada CCD and iTEM (Olympus) software.

Confocal and Ring-TIRF OMX imaging

Confocal imaging was carried out on a Leica TCS SP5 scanning confocal microscope equipped with a 488 nm and 633 nm excitation lasers and Avalanche photodiodes (APDs) for detection.

TIRF time-lapses were acquired on the OMX version 3 system (Applied Precision) using a TIRF 60x APON 1.49NA oil immersion objective lens (Olympus, Center Valley, PA) and CoolSNAP HQ2 CCD cameras with a pixel size of 0.160µm (Photometrics, Tucson, AZ) on). The microscope is equipped with 488-, 561-, and 642-nm solid-state lasers (Coherent and MPB communications). The Ring-TIRF/PK illumination module on the microscope controls the position and rotates the laser beam within the back focal plane of the objective with a high-speed (300Hz) galvanometer to generate a highly uniform TIRF illumination. In addition, this module allows the adjustment of the beam rotation to control the TIRF depth of penetration.

Estimate of the ARF1^{EN}-Halo optical flow

To explore the directionality of ARF-coated tubule motion around the Golgi we used optical flow. We took the following steps:

1) we performed Gaussian smoothing (sigma=0.5 pixels) of the input images to reduce noise,

2) we performed local background subtraction using a white-tophat operation with a radius of 15,

3) we calculated optical flow between consecutive pairs of image frames using a regularized version of the algorithm described in (Fleet and Weiss, 2006)(our concrete implementation can be found at https://bitbucket.org/david_baddeley/python-microscopy/src/default/PYME/Analysis/optic_flow.py).

4) We calculated a Euclidean distance transform from a thresholded mask of the Golgi, yielding an image in which each pixel contained it's distance from the Golgi border. By taking the (numerical) gradient of this distance image we generated a vector for each pixel, which indicated the direction away from the Golgi.

5) We projected the flow vectors obtained in 3 onto this normalized outward direction vector to calculate the component of motion which was directed away from the Golgi.

6) We generated a mask (with a threshold set at half the maximum of the background-subtracted ARF signal) to separate those pixels belonging to tubules and other ARF positive structures from the background

7) For each of several radial bins representing different distances from the Golgi, we separately summed the +ve (outward) flow and the total (absolute value) flow for pixels within our mask. By expressing the outward flow as a fraction of the total flow, we show that there is a net excess outward flow for most radial bins, and that this is particularly pronounced between ~ 3 and 8 μm from the Golgi. Our analysis was implemented using custom python code within the python-microscopy package (http://david_baddeley.bitbucket.org/python-microscopy), and taking advantage of the numpy, scipy, and scikits-image libraries.

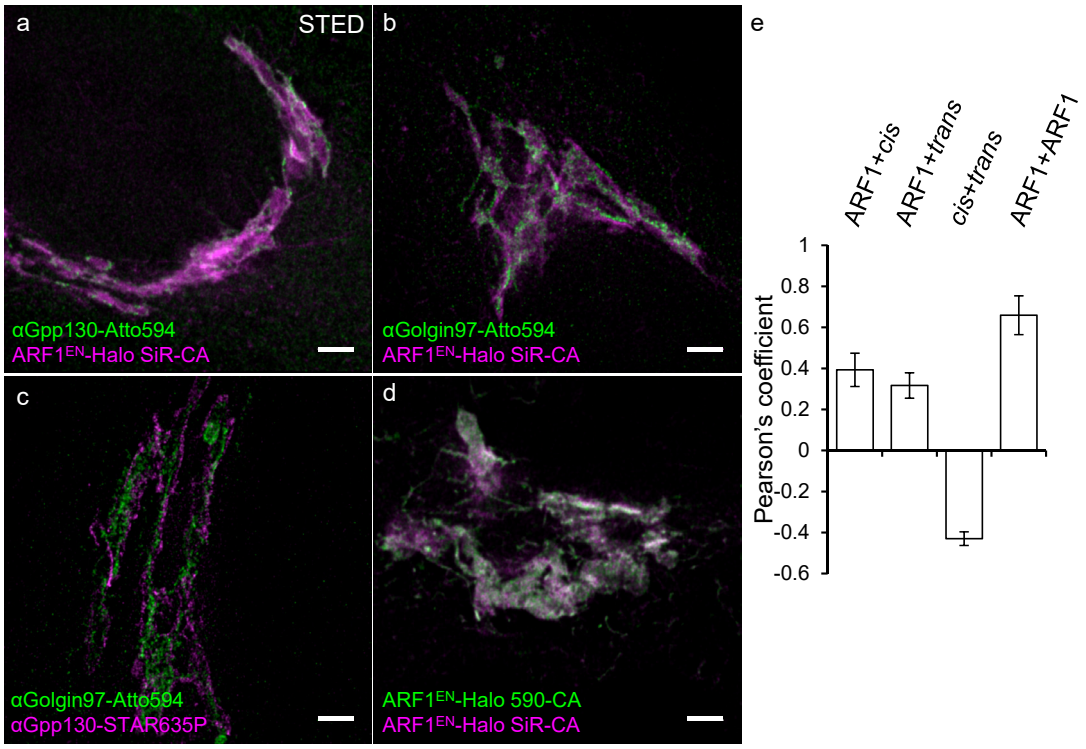

Supplementary Figure 1: ARF1^{EN}-Halo localizes throughout the Golgi stack. ARF1^{EN}-Halo cells were labeled with SiR-CA (a-b) and then fixed with 3% paraformaldehyde and 0.1% glutaraldehyde. Immunofluorescence was carried out with anti-Gpp130 (*cis*-Golgi) (a) and anti-Golgin97 (*trans*-Golgi) (b) and secondary antibodies conjugated to Atto594. As negative control, wt HeLa cells were probed with both anti-Gpp130 and anti-Golgin97 antibodies and secondary antibodies conjugated to Atto590 and STAR635P (c). As positive control, ARF1^{EN}-Halo cells were labeled with both SiR-CA and 590-CA and then fixed as above (d). STED imaging was performed on a custom built setup. ARF1^{EN}-Halo partially co-localizes with both *cis* and trans Golgi markers (n=10 cells for each imaging condition)(e). All STED images were deconvolved, while Pearson's coefficients were calculated on the raw image data. Error bars represent s.d. Scale bars are 2 µm.

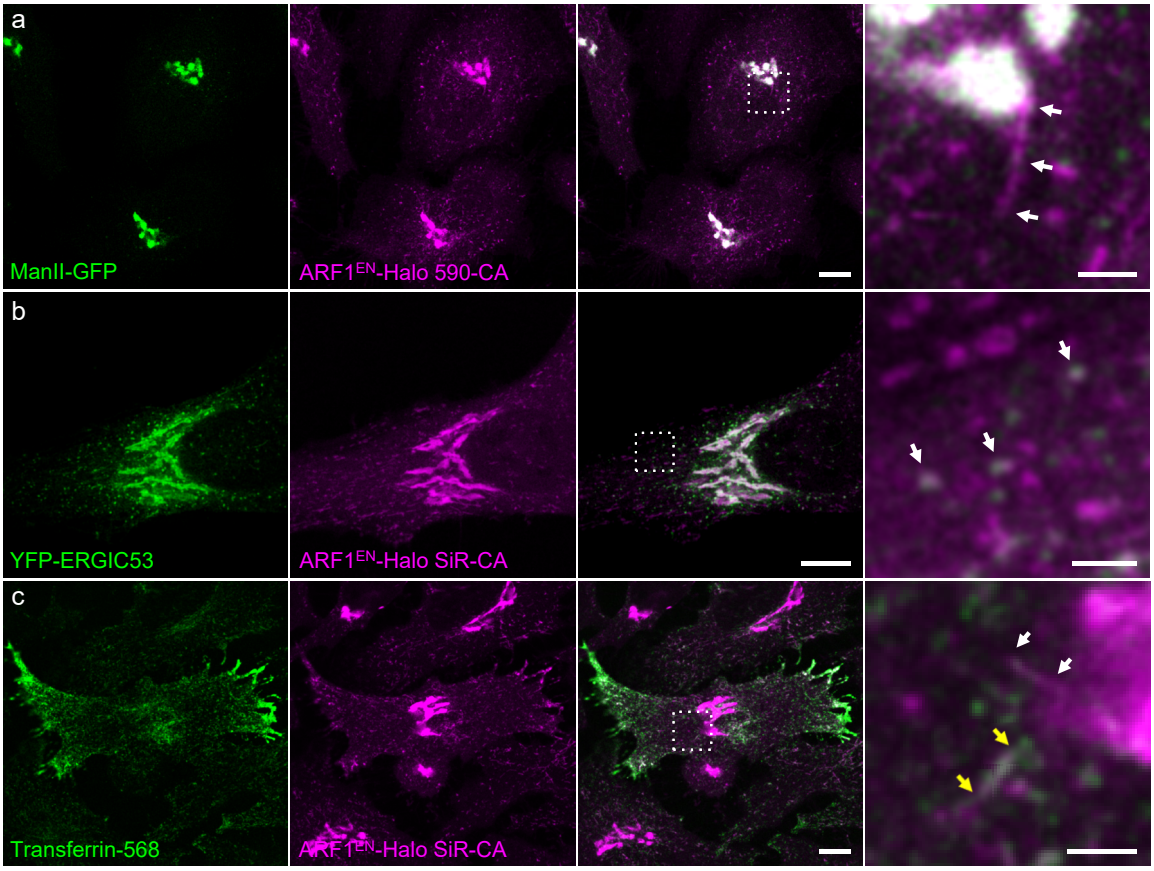

Supplementary Figure 2: Peripheral ARF1^{EN}-Halo structures are ER-Golgi intermediate compartments (ERGIC) and recycling endosomes. ARF1^{EN}-Halo cells were transfected with plasmids encoding for MannosidaseII-GFP (ManII-GFP; a), YFP-ERGIC53 (b) and loaded with Transferrin-568 as described in the methods (c). Cells were then labeled with SiR-CA for confocal imaging. (a) ARF1^{EN}-Halo localizes to the main Golgi body and Golgi-derived tubules (arrows). (b) Peripheral ERGIC structures labeled by both ARF1^{EN}-Halo and YFP-ERGIC53 are highlighted by arrows. (c) Peripheral ARF1^{EN}-Halo tubules contain Transferrin-568 (white arrows) while Golgi-derived tubules (white arrows) do not. Scale bars are 10 µm and 2 µm in the cropped images.

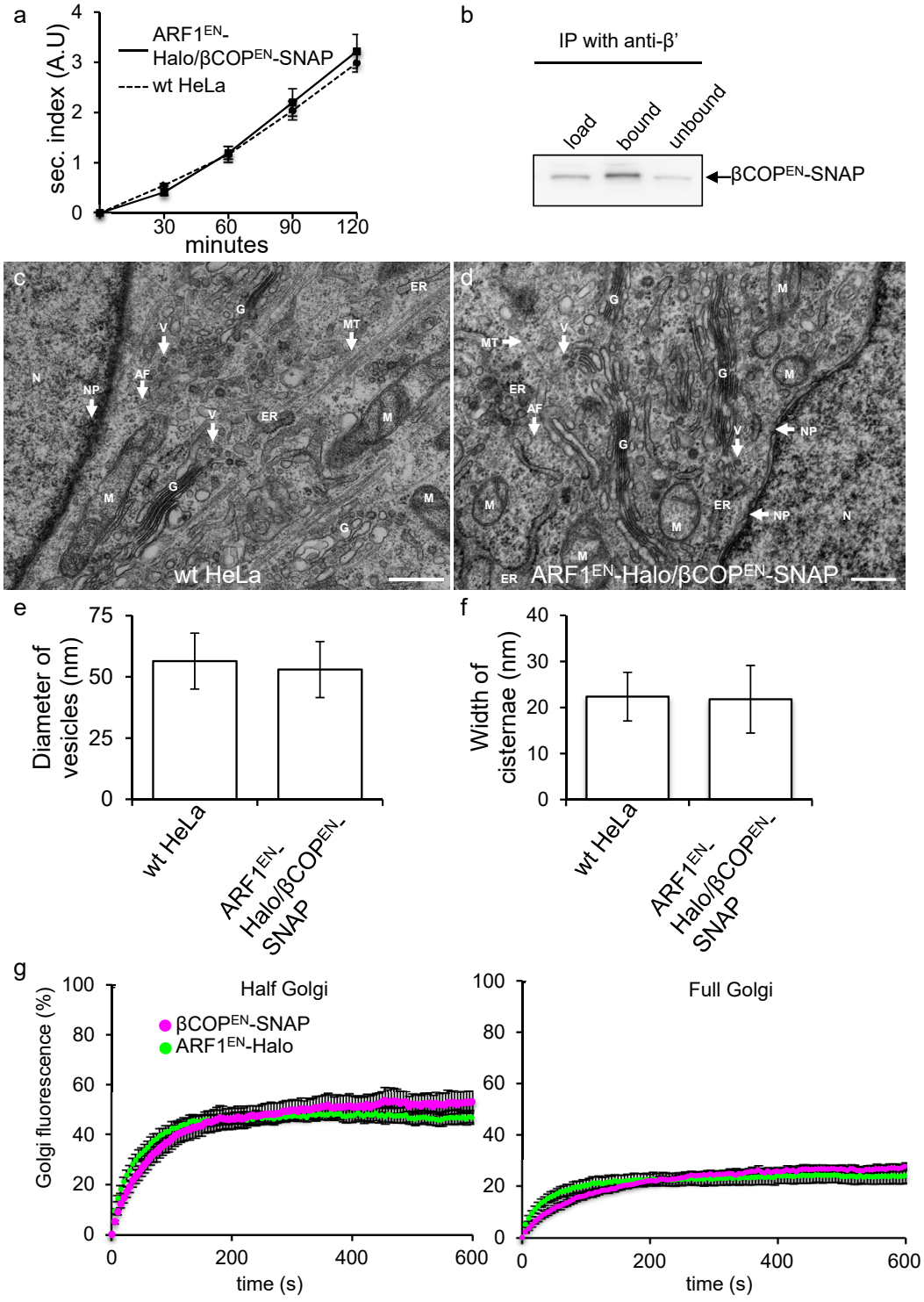

Supplementary Figure 3: The ARF1^{EN}-Halo/βCOP^{EN}-SNAP cell line does not show any functional or morphological defects. Figure legend in the next page.

(a) ARF1^{EN}-Halo/βCOP^{EN}-SNAP and CCL-2 HeLa cells were transfected with a secHRP encoding-plasmid and secHRP secretion was monitored over a period

of 120 minutes. No secretion defects are observed in the gene edited cell line. (b) Pull-down experiment using an antibody that recognizes the β' subunit of the Coatomer complex. β'-COP co-precipitates βCOP^{EN}-SNAP suggesting successful incorporation in the Coatomer complex. (c-d) Electron microscopy shows no morphological alterations of the gene edited cell lines. We observed no changes in the diameter of vesicles (e) or width of the cisternae (f). (g) Fluorescence recovery after photobleaching (FRAP) experiments show recovery of ARF1^{EN}-Halo and β-COP^{EN}-SNAP with a half-time of 28.90 ± 2.9 seconds and 54.7 ± 7.69 seconds respectively when only half of the Golgi was bleached. When the whole Golgi area was bleached ARF1^{EN}-Halo and β-COP^{EN}-SNAP recovered with a half time of 29.56 ± 2.58 seconds and 75.57 ± 9.9 seconds respectively. AF: Actin Filament, ER: Endoplasmic Reticulum, G: Golgi, M: Mitochondria, MT: Microtubules, N: Nucleus, NP: Nuclear Pore, V: Vesicle. Error bars represent s.d. (a,e-f) and s.e.m (g). Scale bars in (c) and (d) are 500 nm.

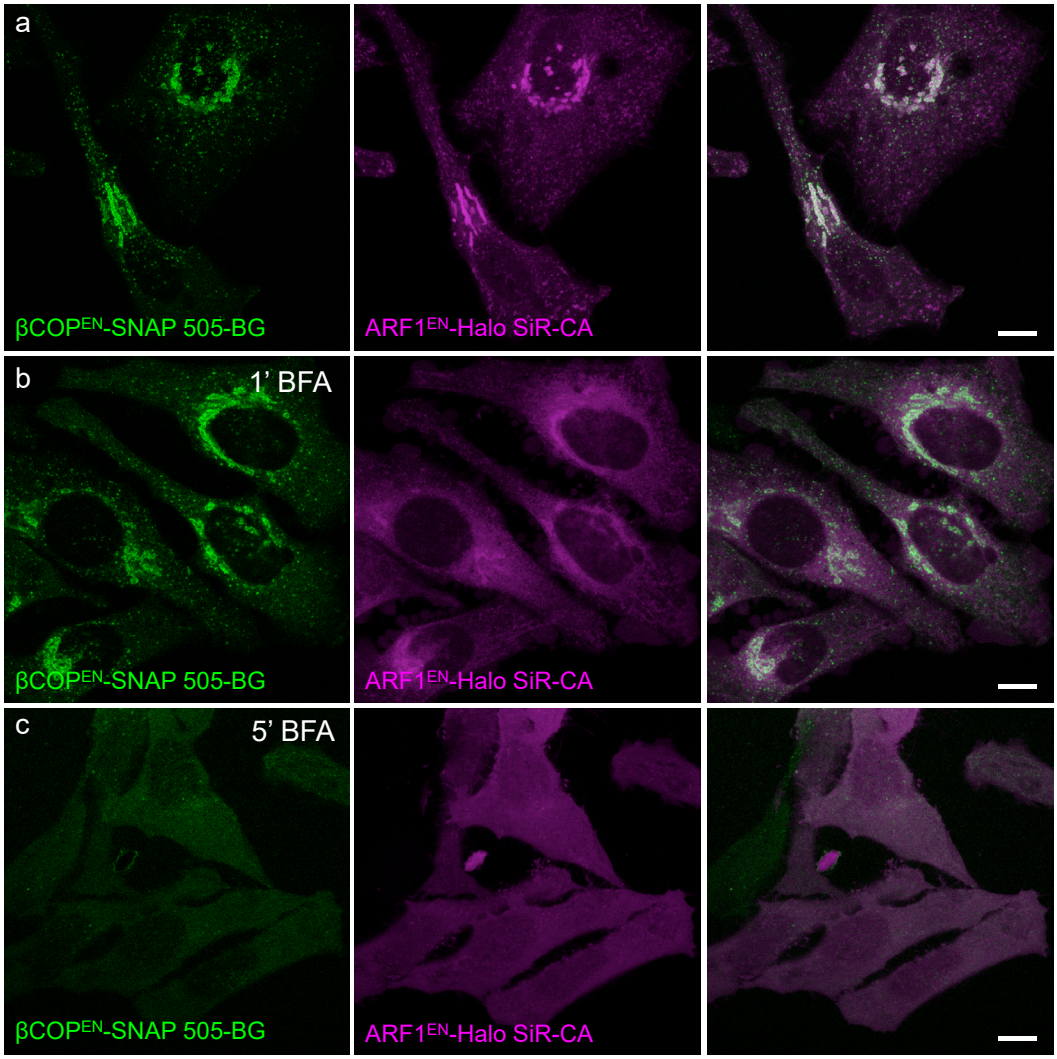

Supplementary Figure 4: ARF1^{EN}-Halo and βCOP^{EN}-SNAP are Brefeldin A-sensitive. ARF1^{EN}-Halo/βCOP^{EN}-SNAP cells were labeled with SiR-CA and 505-BG. BFA was added to cells at a concentration of 100 µg/ml. (b) 1 minute after addition of BFA, βCOP^{EN}-SNAP is still associated with the Golgi while ARF1^{EN}-Halo has almost fully redistributed to the cytosol. (c) 5 minutes after addition of BFA, all cells show only cytoplasmic staining for both markers. Scale bars are 10 µm.

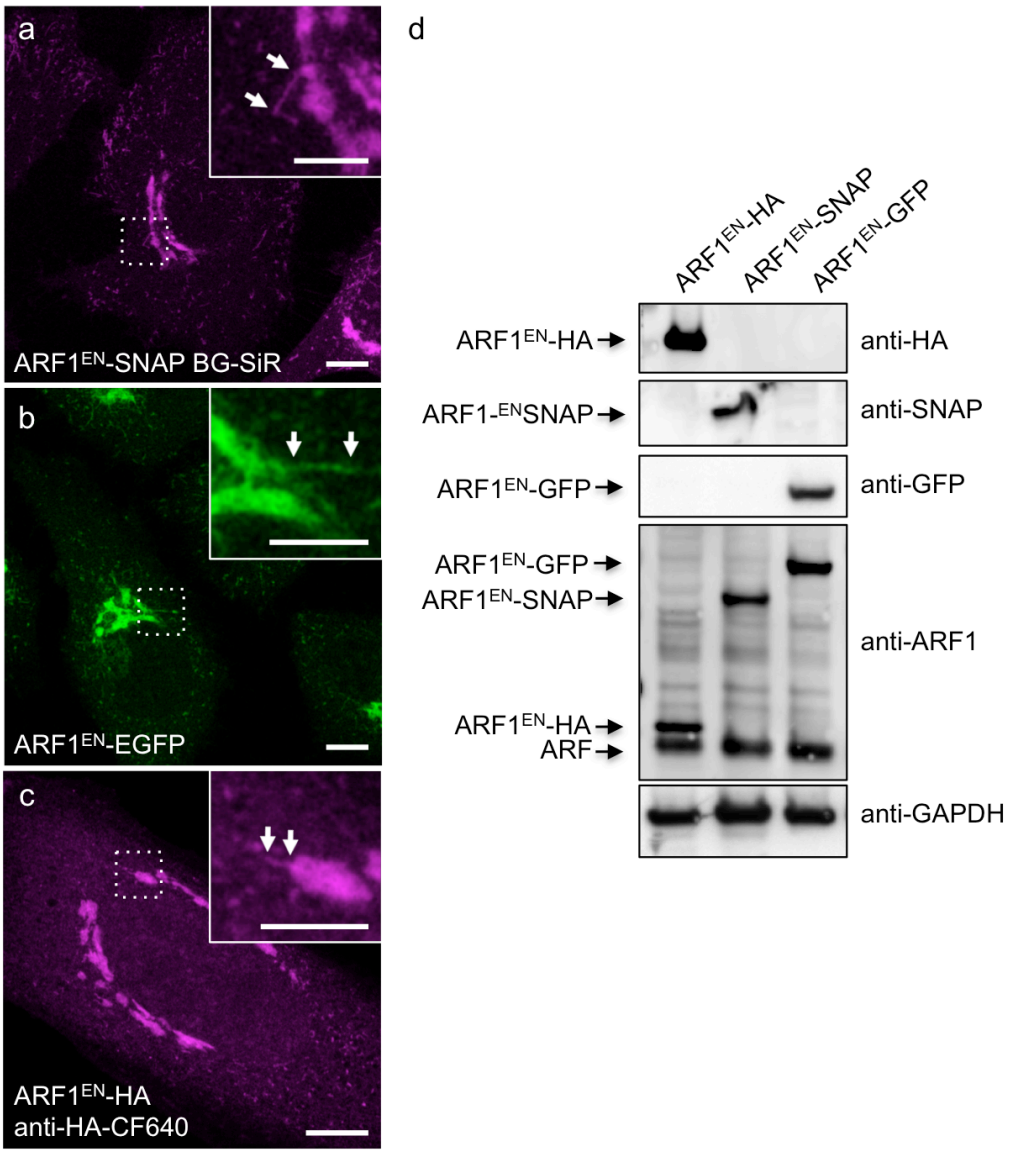

Supplementary Figure 5: CRISPR cell lines with different tags show the same phenotype of ARF1^{EN}-Halo. CCL-2 HeLa cells were edited as described in the supplementary methods to generate ARF1^{EN}-SNAP (a) and ARF1^{EN}-EGFP and ARF1^{EN}-HA (c). Live-cell imaging highlights Golgi-derived tubular structures (arrows) for both the ARF1^{EN}-SNAP and ARF1^{EN}-EGFP cell lines. A strong fixation with 3% PFA and 0.1% glutaraldehyde allows partial preservation of tubules decorated by ARF1^{EN}-HA (c). Western blot analysis shows the correctly tagged fusion proteins (d). Scale bars are 10 µm and 5 µm in the cropped images.

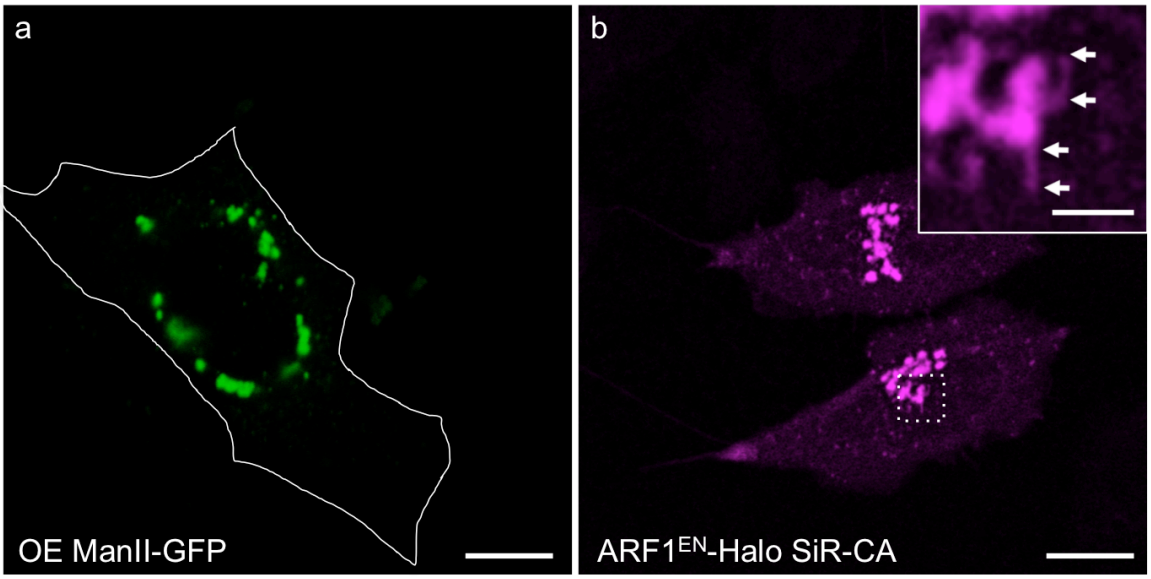

Supplementary Figure 6: Gene editing of the haploid cell line HAP1 reveals tubules decorated by ARF1^{EN}-Halo. HAP1 cells were transfected with the Golgi marker MannosideII-GFP (ManII-GFP) to reveal the morphology of the Golgi apparatus (a). Our method for gene-editing HeLa CCL-2 cells was repeated using HAP1 cells. ARF1^{EN}-Halo decorated Golgi-derived tubular structures (arrows) in live-cell imaging experiments (b). Scale bars are 10 μm and 2 μm in the cropped image.

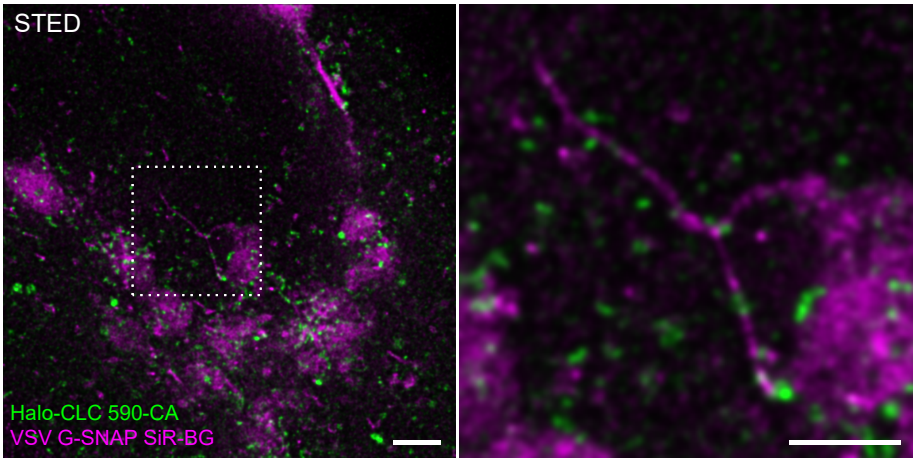

Supplementary Figure 7: Live-cell STED imaging highlights that VSV G-SNAP-containing tubules are decorated by Clathrin clusters. HeLa cells were electroporated with Halo-CLC and VSV G-SNAP encoding-plasmids and incubated overnight at 40.5 °C. Cells were then labeled with 590-CA and SiR-BG. Release of VSV G-SNAP from the ER was trigged by transferring cells to a stage-top incubator heated at 32 °C. ~ 30 minutes after release, we observed VSV G-SNAP-positive tubules decorated by Clathrin clusters emanating from the Golgi (arrows in cropped image). All STED images were deconvolved. Scale bars are 2 µm and 1 µm in the cropped image.

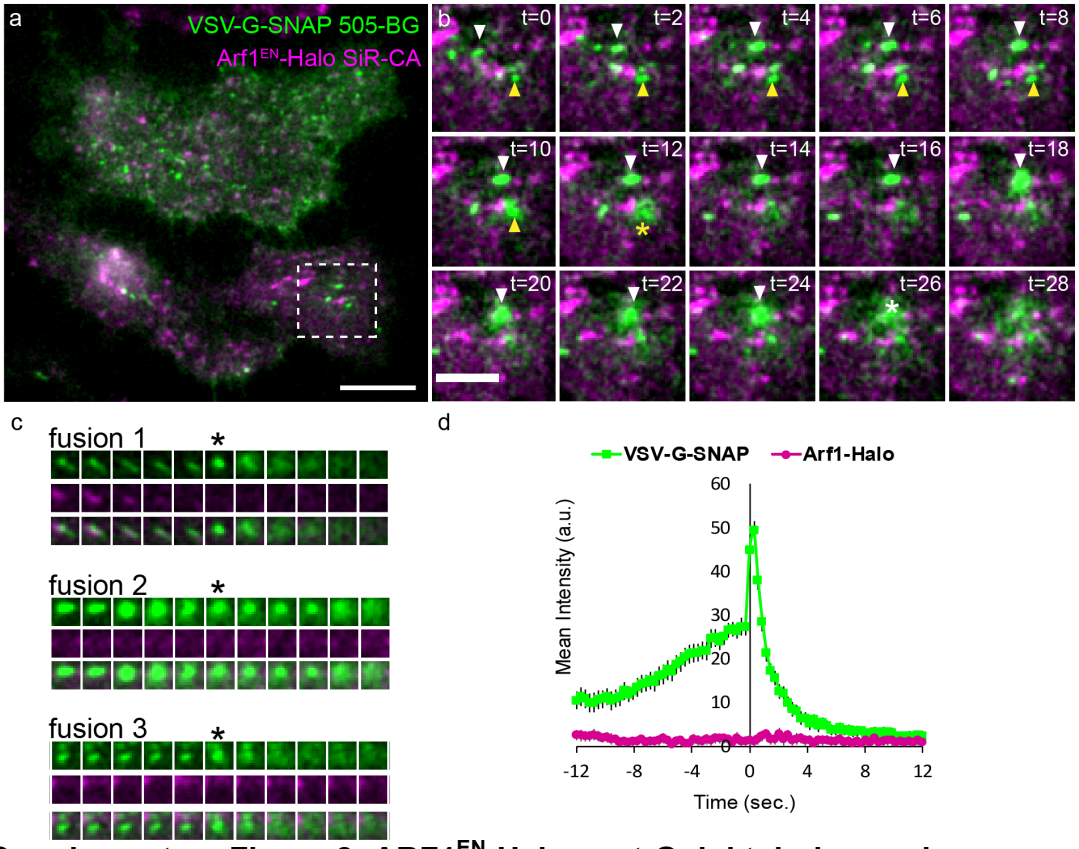

Supplementary Figure 8: ARF1^{EN}-Halo post-Golgi tubular carriers never fuse with the plasma membrane. ARF1^{EN}-Halo cells were electroporated with a VSV G-SNAP encoding-plasmid and incubated overnight at 40.5 °C. Cells were then labeled with SiR-CA and 505-BG for TIRF imaging (a). Release of VSV G-SNAP from the ER was trigged by transferring cells to a stage-top incubator heated at 32 °C. ~30-45 minutes after release we started observing VSV G-SNAP positive structures docking and fusing with the plasma membrane (b; two examples are highlighted with white and yellow arrowheads). All the structures monitored did not contain ARF1^{EN}-Halo. Examples of fusion events of VSV-G-SNAP positive carriers (c). Graph representing the average of 72 fusion events in 6 different cells (d). Error bars are s.e.m. Scale bars are a=10 μm and b=5 μm.

	# of fluorescent molecule of standard	ratio ARF1-Halo/standard	# estimated ARF1 molecules (per µm of tube length)	**ARF1 density (per µm^2)**
in vitro COPI (cryo-EM) (Dodonova et al., 2015)	-	-	-	~20,000 (50.4 nm/ARF1 molecule)
this publication (COPI standard)	150 β-COP^{EN}-SNAP/vesicle	2.2±1.5	~3300	~10,000 (104 nm/ARF1 molecule)
this publication (tubulin standard)	1750 tubulin subunits/µm of microtubule length (Cooper et al., 2010)	2.1±0.7	~7350	~20,000 (47 nm/ARF1 molecule)

Supplementary Table 1: Estimate of the density of ARF1 molecules on the tubules. Using COPI vesicles and microtubules as internal standards we estimate the density of ARF1 on the tubules to be ~10,000-20,000 ARF1/µm^2. This is similar to what has been observed for *in vitro* generated COPI vesicles (Dodonova et al., 2015). Supplementary Information Note 1 contains a more detailed explanation of the calculations.

Legends for Supplementary Videos

Supplementary Video 1: Confocal imaging of ARF1^{EN}-Halo cells labeled with SiR-CA. Scale bar is 10 µm.

Supplementary Video 2: Two-color live-cell STED imaging of SNAP-CLC labeled with SiR-CA (magenta) and ARF1^{EN}-Halo labeled with 590-CA (green). Scale bar is 2 µm.

Supplementary Video 3: Confocal imaging of ARF1^{EN}-Halo labeled with SiR-CA (magenta) and VSV G-SNAP labeled with 505-BG (green). Scale bar is 10 µm.

Supplementary Video 4: deep-TIRF imaging of ARF1^{EN}-Halo labeled with SiR-CA (magenta) and β-COP^{EN}-SNAP labeled with 505-BG (green). Scale bar is 2 µm.

Supplementary Video 5: Two-color live-cell STED imaging of ARF1^{EN}-Halo labeled with 590-CA (green) and β-COP^{EN}-SNAP labeled with SiR-BG (magenta). Scale bar is 2 µm.

Supplementary Video 6: Confocal imaging of ARF1^{EN}-Halo labeled with SiR-CA (magenta) and KDEL-R-SNAP labeled with 505-BG (green). Scale bar is 5 µm.

References

Barlowe, C., and Helenius, A. (2016). Cargo Capture and Bulk Flow in the Early Secretory Pathway. Annu Rev Cell Dev Biol *32*, 197-222.

Barlowe, C., Orci, L., Yeung, T., Hosobuchi, M., Hamamoto, S., Salama, N., Rexach, M.F., Ravazzola, M., Amherdt, M., and Schekman, R. (1994). CopII - a membrane coat formed by Sec proteins that drive vesicle budding from the endoplasmic-reticulum. Cell *77*, 895-907.

Bottanelli, F., Kromann, E.B., Allgeyer, E.S., Erdmann, R.S., Wood Baguley, S., Sirinakis, G., Schepartz, A., Baddeley, D., Toomre, D.K., Rothman, J.E.*, et al.* (2016). Two-colour live-cell nanoscale imaging of intracellular targets. Nat Commun *7*, 10778.

Cong, L., Ran, F.A., Cox, D., Lin, S.L., Barretto, R., Habib, N., Hsu, P.D., Wu, X.B., Jiang, W.Y., Marraffini, L.A.*, et al.* (2013). Multiplex Genome Engineering Using CRISPR/Cas Systems. Science *339*, 819-823.

Connolly, C.N., Futter, C.E., Gibson, A., Hopkins, C.R., and Cutler, D.F. (1994). Transport into and out of the Golgi complex studied by transfecting cells with cDNAs encoding horseradish peroxidase. The Journal of cell biology *127*, 641-652.

Cooper, J.R., Wagenbach, M., Asbury, C.L., and Wordeman, L. (2010). Catalysis of the microtubule on-rate is the major parameter regulating the depolymerase activity of MCAK. Nat Struct Mol Biol *17*, 77-82.

Deng, Y., Rivera-Molina, F.E., Toomre, D.K., and Burd, C.G. (2016). Sphingomyelin is sorted at the trans Golgi network into a distinct class of secretory vesicle. Proc Natl Acad Sci U S A *113*, 6677-6682.

Dodonova, S.O., Diestelkoetter-Bachert, P., von Appen, A., Hagen, W.J., Beck, R., Beck, M., Wieland, F., and Briggs, J.A. (2015). VESICULAR TRANSPORT. A structure of the COPI coat and the role of coat proteins in membrane vesicle assembly. Science *349*, 195-198.

Fleet, D.J., and Weiss, Y. (2006). Optical flow estimation. Handbook of Mathematical Models in Computer Vision, 237-257.

Hamlin, J.N., Schroeder, L.K., Fotouhi, M., Dokainish, H., Ioannou, M.S., Girard, M., Summerfeldt, N., Melancon, P., and McPherson, P.S. (2014). Scyl1 scaffolds class II Arfs to specific subcomplexes of coatomer through the gamma-COP appendage domain. J Cell Sci *127*, 1454-1463.

Mali, P., Yang, L., Esvelt, K.M., Aach, J., Guell, M., DiCarlo, J.E., Norville, J.E., and Church, G.M. (2013). RNA-guided human genome engineering via Cas9. Science *339*, 823-826.

Presley, J.F., Cole, N.B., Schroer, T.A., Hirschberg, K., Zaal, K.J., and Lippincott-Schwartz, J. (1997). ER-to-Golgi transport visualized in living cells. Nature *389*, 81-85.

Thor, F., Gautschi, M., Geiger, R., and Helenius, A. (2009). Bulk flow revisited: transport of a soluble protein in the secretory pathway. Traffic *10*, 1819-1830.

Vasudevan, C., Han, W., Tan, Y., Nie, Y., Li, D., Shome, K., Watkins, S.C., Levitan, E.S., and Romero, G. (1998). The distribution and translocation of the G protein ADP-ribosylation factor 1 in live cells is determined by its GTPase activity. J Cell Sci *111 (Pt 9)*, 1277-1285.